JOURNAL OF SOLID STATE CHEMISTRY 117, 8–15 (1995)

FT-IR Skeletal Powder Spectra of Ba-β-Aluminas with Compositions $BaAl_9O_{14.5}$, $BaAl_{12}O_{19}$, and $BaAl_{14}O_{22}$ and of Ba-Ferrite, $BaFe_{12}O_{19}$

Maurizio Bellotto,* Guido Busca,†,1 Cinzia Cristiani,‡ and Gianpiero Groppi‡

*CISE, P.O. Box 12081, 20134 Segrate, Milan, Italy; †Istituto di Chimica, Facoltà di Ingegneria, Università, P.le Kennedy, I-16129 Genoa, Italy; and ‡Dipartimento di Chimica Industriale e Ingegneria Chimica "G. Natta," Politecnico di Milano, P. L.DaVinci 22, I-20123 Milan, Italy

Received July 13, 1994; in revised form October 17, 1994; accepted October 19, 1994

The FT-IR/FT-FIR powder skeletal spectra of β-aluminas of composition $BaAl_9O_{14.5}$, $BaAl_{12}O_{19}$, and $BaAl_{14}O_{22}$ and of a magnetoplumbite-type Ba-ferrite $BaFe_{12}O_{19}$ are reported and discussed, on the basis of the structural models previously proposed for these solids. These models find good confirmation in such skeletal spectra. Emphasis is focused on the defect structure of these compounds.

INTRODUCTION

β-aluminas have been the object of attention mainly because of their ionic conduction properties. This is a family of compounds usually with the general formula $M_2O \cdot nAl_2O_3$, where M is a large monovalent cation (1). The stoichiometry of "ideal" Na-β-alumina is $NaAl_{11}O_{17}$ (2, 3), with $n = 11$ in the above general formula, although Na excess is frequently present. Its layered structure is constituted by spinel-type blocks having the formula $[Al_{11}O_{16}]^+$ separated by mirror planes where mobile Na^+ ions are located together with oxygens bridging between spinel blocks.

Similar structures can also be exhibited by aluminates of divalent and trivalent metals, if the cationic radius is sufficiently high, as for Ba^{2+}, Pb^{2+}, and La^{3+} (4–6). In the case of Ba-β-alumina, two different structures have been reported, the so-called Ba-poor structure, whose stoichiometry is near $0.82\ BaO \cdot 6\ Al_2O_3$ (7), and the so-called Ba-rich structure with a stoichiometry near $1.31\ BaO \cdot 6\ Al_2O_3$ (8).

Ba-β-aluminate (9) and La-β-aluminate powders (10) have recently been described as ceramic materials very resistant to sintering. For this reason, they have been proposed for the formulation of catalysts for hydrocarbon combustion. Similar ion-conducting structures are known also for ferrites, such as K-β-ferrite $KFe_{11}O_{17}$ (11), and for gallates as well.

When the ratio between the ionic radii of the bivalent and trivalent cations decreases (i.e., for smaller bivalent cations or larger trivalent ions (1, 4)), the alternative non-ion-conducting megnetoplumbite-type structures are formed, as in the cases of $CaAl_{12}O_{19}$, $SrAl_{12}O_{19}$, $BaFe_{12}O_{19}$, and $PbFe_{12}O_{19}$. $BaFe_{12}O_{19}$ is the object of deep investigation today because of its industrial application as a hard anisotropic ferrimagnetic material (12).

Mixed magnetoplumbite/β-alumina structures have been found in compounds such as Na–La mixed aluminates (13), K–Ba mixed ferrites (14) and $BaAl_6Fe_6O_{19}$ (15), thus showing the "flexibility" of these closely related hexagonal structures.

The preparation (16), the solid state chemistry (17), and the surface properties (18) of Ba-β-alumina powders have been investigated previously. We report here a further solid state investigation of these materials, and, for comparison, of a magnetoplumbite-type compound, $BaFe_{12}O_{19}$, using IR skeletal spectroscopy.

EXPERIMENTAL

(*a*) *Preparation of the samples.* Ba-Al-O samples with nominal atomic ratio Al/Ba = 9, 12, and 14 (hereafter denoted BaAl9, BaAl12, and BaAl14) were prepared according to the precipitation method in aqueous medium, as reported in Ref. (16). $Ba(NO_3)_2$ (Fluka) was completely dissolved in hot water (T = 330 K) under vigorous stirring. The resulting solutions were acidified (pH = 1) with HNO_3 and subsequently $Al(NO_3)_3 \cdot 9\ H_2O$ (Fluka 98%) was added to them. The mixtures were poured, under vigorous stirring and constant temperature (T = 330 K), into solution of $(NH_4)_2CO_3$. The formation of white precipitates were observed. The slurries were then aged at 330 K for about 3 hr; the pH of the slurry varied in the range 7.5–8. The precipitates were filtered, washed, and dried overnight at 330 K. Analysis by atomic absorption for Ba and Al content in mother liquors and washing waters indicated that the precipitation occurred in a quantitative way. Chemical analysis of the dried samples confirmed that the actual Al/Ba ratios

0022-4596/95 $6.00

closely correspond to the nominal ones. The precursors dried at 370 K were ground to between 150 and 200 mesh and were calcined at 1670 K according to the following calcination procedures: steps at 470, 770, 970, 1170, 1270, 1370, 1470, 1570 and 1670 K, heating rate for each step 60 K/hr; holding 10 hr; cooling rate 100 K/hr. No grinding of the samples was performed after each calcination.

Ba ferrite (Fe/Ba ratio = 12) was prepared using an analogous procedure.

(*b*) *Characterization of the samples.* XRD analyses were performed by a Philips PW 1050-70 vertical goniometer using Ni-filtered Cu$K\alpha$ radiation. A typical experiment was performed in the range 5–130° 2θ, step size 0.002° 2θ, 10 sec/step, and divergent slit 0.25° 2θ. The FT-IR spectra were recorded using a Nicolet Magna 750 Fourier transform instrument. For the region 4000–350 cm^{-1} a KBr beam splitter was used with a DTGS detector, while for the FIR region (600–50 cm^{-1}) a "solid substrate" beam splitter and a DTGS polyethylene detector have been used. KBr pressed disks (IR region) or polyethylene pressed disks and samples deposed on Si disks (FIR region) were used.

RESULTS AND DISCUSSION

As discussed in detail previously (16), XRD analyses showed that the samples BaAl14 and BaAl9 are constituted by the Ba-poor and the Ba-rich Ba-β-alumina phases, respectively (JCPDS Tables 33-128 and 33-129), while the diffraction pattern of the BaAl12 sample has been interpreted as an intergrowth of the two Ba-β-alumina phases. The Ba ferrite sample is well crystallized in the magnetoplumbite-type structure (JCPDS Tables 27-1029 and 39-1433).

The IR and FIR spectra of our Ba-β-alumina powders (BaAl9, BaAl12, and BaAl14) are reported in Figs. 1 and 2. In Fig. 3 the spectra of a spinel-type alumina predominantly constituted by θ-Al_2O_3 and of the aluminate with the inverse spinel structure $NiAl_2O_4$ are also reported for comparison. In Fig. 4 the skeletal spectra of $BaFe_{12}O_{19}$ and of the spinel-type oxides γ-Fe_2O_3 (maghemite) and $ZnFe_2O_4$ (franklinite) are also compared.

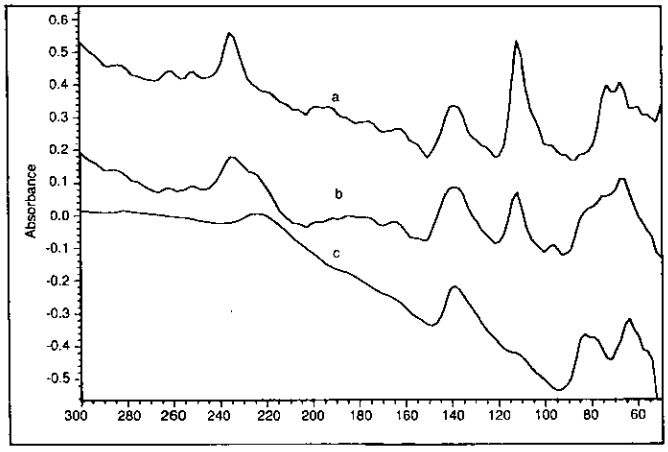

FIG. 2. FT-IR/FT-FIR skeletal spectra of (a) BaAl9, (b) BaAl12, and (c) BaAl14: modes associated with vibrations of the atoms lying in the "mirror planes".

According to the large dimensions of the unit cell of β-aluminas, their skeletal spectra present a large number of sharp maxima. The positions of these maxima are summarized in Table 1, where they are compared with the positions of the maxima reported in the literature for the IR spectra of other β-aluminas.

An interpretation of these skeletal IR spectra can be attempted on the basis of the known structure of the corresponding materials. The unit cell dimensions of these phases are reported in Table 2. The atom positions in the hexagonal mixed oxides are compared in Table 3.

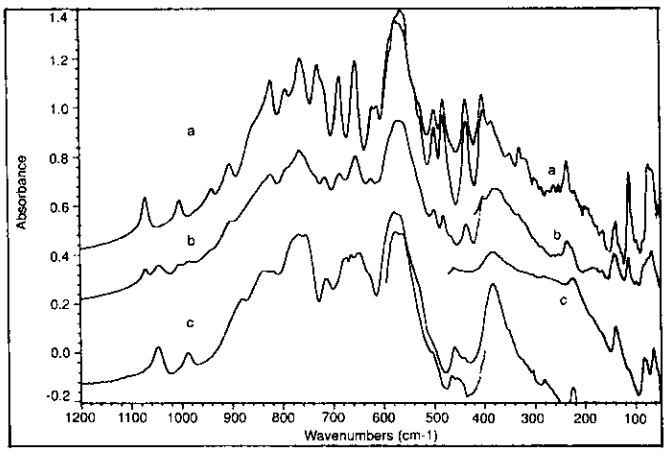

FIG. 1. FT-IR/FT-FIR skeletal spectra of (a) BaAl9, (b) BaAl12, and (c) BaAl14.

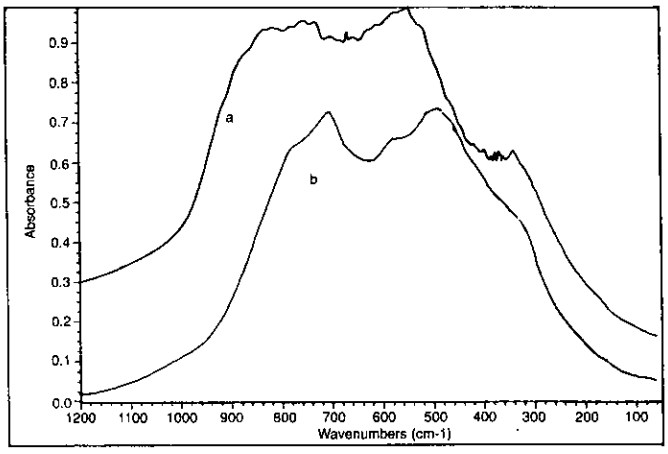

FIG. 3. FT-IR/FT-FIR skeletal spectra of Θ/δ-Al_2O_3 (a defective spinel-type phase) and $NiAl_2O_4$ (an inverse aluminate spinel).

TABLE 1
Position (cm^{-1}) of the IR Bands in β-Aluminas

Ba-β-Al_2O_3			Na-β-Al_2O_3			Ag-β-Al_2O_3		Assignments	
BaAl9 tr, p	BaAl12 tr, p	BaAl14 tr, p	refl, m a	refl, m b	tr, p c	refl, m b	tr, p c	a, c	this work
1071	1072	—							
—	1045	1047	1060	1115		1045		A_{2u}	
1003	1004								
—	986	987							
940	942s	—	920	882		900		E_{1u}	
903	901s	880	890					A_{2u}	
860s		840	865	854		860		A_{2u}	
821	822	820	825	820		820		E_{1u}	
792		767	777	780		767		A_{2u}	
762	764	758	768	758		762		E_{1u}	
755									
728			720	750		720		A_{2u}	
720s	715	712	718	702				E_{1u}	
684	685	672	670	658		682		E_{1u}	spinel blocks
653	653	660	640	667		643		A_{2u}	
620	623	647	630	627		645		E_{1u}	
611		614s	590	590		582		E_{1u}	
570		575	555	558		555		E_{1u}	
560	565	560	530	555		535		A_{2u}	
540									
498	499	500s	500	506		505		E_{1u}	
480	480	460	445	450		452		E_{1u}	
435	434	455	435	440		432		A_{2u}	
402	400		390	395		397		A_{2u}	
384	379	382	387					E_{1u}	
			373	365		367		E_{1u}	
350	347		337	342		341		A_{2u}	
328	331		310	325		323		A_{2u}	
318	315s		307	306		304		E_{1u}	
300	300s		302					E_{1u}	
283	285s	281	295	313		308		A_{2u}, E_{1u}	
235	234							A_{2u}	
	224s	224	287		270		274	A_{2u}	bridging
138	139	138		212	211	212	215	E_{1u}	oxygen
111, 105	112,105							—	Interstitial Ba
	82	82		105	126	87	105	A_{2u}	
73	75					66		A_{2u}	conducting ions
67	67	64		61	60	29	30	E_{1u}	

Note. a = Ref. (19); b = Ref. (20); c = Ref. (22); tr, p = transmission, powders; refl, m = reflection, monocrystals.

TABLE 2
Hexagonal Unit Cell Dimensions (Å) of Na- and Ba-β-Aluminas and of Ba Ferrite

Compound	Formula	a	c	Ref.
Na-β-alumina	$NaAl_{11}O_{17}$	5.594	22.53	(2)
Ba-poor Ba-β-alumina	$Ba_{0.75}Al_{11}O_{17.25}$	5.582	22.715	(7)
Ba-rich Ba-β-alumina	$Ba_{1.16}Al_{10.67}O_{17.16}$	5.600	22.922	(8)
Ba-ferrite	$BaFe_{12}O_{19}$	5.892	23.183	(21)

The structure of Na-β-alumina, of the Ba-poor Ba-β-alumina sample, and of $BaFe_{12}O_{19}$ have been determined in detail. All belong to the $P6_3/mmc = D^4_{6h}$ space group, with two formula units per unit cell, and with a close correspondence between the respective unit cells. As for the Ba-rich β-alumina structure, single crystal studies suggested that it belongs to the space group $P\bar{6}m2 = D^1_{3h}$, which corresponds to the $P6_3/mmc$ space group of the other structures but without the inversion center and the

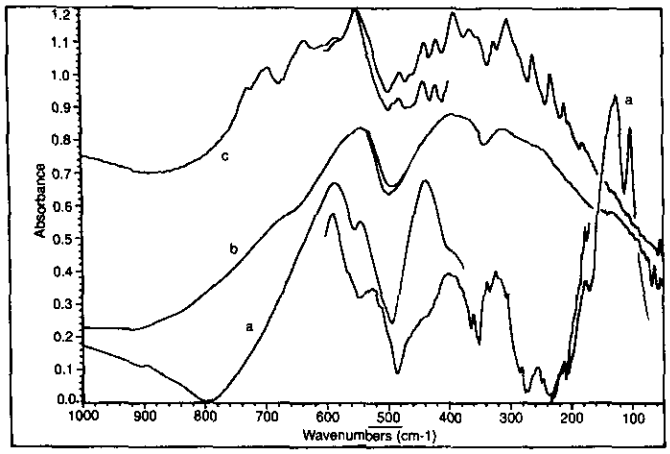

FIG. 4. FT-IR/FT-FIR skeletal spectra of (a) $BaFe_{12}O_{19}$, (b) $ZnFe_2O_4$, and (c) γ-Fe_2O_3.

c glide plane. This comes about from the particular defective structure it exhibits (see below), and it is an expression of the fact that, for energetic reasons, it is impossible to allocate neighbor Ba ions. Moreover, single crystal data showed that this structure shows an $a\sqrt{3} \times a\sqrt{3}$ superstructure in the *a*, *b* plane, which is completely disordered along the *c* direction (8). This feature again arises from the higher energy associated with an arrangement that encompasses two defective cells as nearest neighbors (i.e., cells containing interstitial sites). However, Rietveld analysis of the XRD powder pattern of this Ba-rich β-alumina sample suggested that it is possible to model its structure on the basis of an average cell which still retains the inversion center and correspondence to the ideal β-alumina unit cell (16).

In the "ideal" structure of Na-β-alumina first determined by Beevers and Ross (2), and successively refined by Peters *et al.* (3), the stoichiometry is $NaAl_{11}O_{17}$. This ideal structure is constituted by "spinel blocks" with four cubic close packed layers of oxide ions with composition $[Al_{11}O_{16}]^+$, separated by other ccp planes ("mirror planes") where three quarters of the oxide ions are missing. Every mirror plane contains one Na^+ cation and one oxide anion (O(5) in Table 2) per unit cell, located on ccp positions.

In the so-called Ba-poor β-alumina phase, whose stoichiometry may be written as $Ba_{0.75}Al_{11}O_{17.25}$, Ba incompletely occupies the Na positions of the ideal $NaAl_{11}O_{17}$ structure (the so-called Beever–Ross or BR position). Such mobile Ba ions have unusually low coordination (9 compared to the more usual 12-fold coordination of Ba^{2+} in mixed oxides) with also an unusually high mean Ba–O distance (2.97 Å compared to 2.80–2.90 Å). To account for neutrality, one-fourth of the Ba ions are missing, and

TABLE 3
Atom Positions, Site Symmetries (sym), Occupancies (occ), and Total Atom Number (*N*) in β-Alumina and Magnetoplumbite-Type Phases

			β-Aluminas						Magnetoplumbite $BaFe_{12}O_{19}$ Ref. 21				
			$NaAl_{11}O_{17}$ Refs. 2, 3		$Ba_{0.75}Al_{11}O_{17.25}$ Ref. 7		$Ba_{1.16}Al_{10.66}O_{17.16}$ Ref. 16		Ideal		Real		
Ion	Site	Site sym.	Occ.	*N*	Occ.	*N*	Occ.	*N*	Occ.	*N*	Occ.	*N*	Location
M'(1)	2d	D_{3h}	1	2	0.75	1.5	0.83	1.66	1	2	1	2	MP
M'(2)	4f	C_{3v}	=	=	=	=	0.16	0.66	=	=	=	=	SB
M''(1)	12k	C_s	1	12	0.91	11	0.83	10	1	12	1	12	SB
M''(2)	4f	C_{3v}	1	4	1	4	0.83	3.33	1	4	1	4	SB
M''(3)	4f	C_{3v}	1	4	1	4	1	4	1	4	1	4	SB
M''(4)	2a	D_{3d}	1	2	1	2	1	2	1	2	1	2	SB
M''(5)	12k	C_s	=	=	0.09	1	0.17	2	=	=	=	=	SB
	2d	D_{3h}	=	=	=	=	=	=	1	2	=	=	MP
	4e	C_{3v}	=	=	=	=	=	=	=	=	0.5	2	near MP
O(1)	12k	C_s	1	12	1	12	1	12	1	12	1	12	SB
O(2)	12k	C_s	1	12	1	12	1	12	1	12	1	12	SB
O(3)	4f	C_{3v}	1	4	1	4	1	4	1	4	1	4	SB
O(4)	4e	C_{3v}	1	4	1	4	0.83	3.33	1	4	1	4	SB
O(5)	2c	D_{3h}	1	2	1	2	1	2	1	2	1	2	MP
O(6)	6h	C_{2v}	=	=	0.09	0.5	0.17	1	1	6	1	6	MP

Note. *M'* = Na or Ba; *M''* = Al or Fe; MP = mirror planes; SB = spinel blocks.

are substituted by an additional oxide ion placed in the so called "middle oxide" (or mO) position (O(6)) (7). This additional oxygen, constituting a "Reidinger defect," is associated with the shift of the two nearest Al ions from an octahedral position (Al(1)) to a tetrahedral position (Al(5)). These defects would occur at random, thus retaining the unit cell dimensions and the space group of Na-β-alumina.

On these bases, we can propose an interpretation of the spectrum of BaAl14 as that of the Ba-poor Ba-β-aluminate, isomorphous to stoichiometric Na-β-alumina, with Ba substituting for Na and random defects (Ba ions lacking and an additional oxide ion) every four mirror planes. Under this assumption, the same number of fundamentals can be expected, with the same symmetries, although absorptions associated to the additional O(6) ions could also be expected. The bands associated with the atoms in the mirror plane (where defects are located) could be broadened, and are expected to be shifted in relation to the different weight, size and charge of Na^+ and Ba^{2+} cations.

The unit cell of Na-β-alumina contains 58 atoms. Thus, it possess 174 degrees of freedom, of which 3 correspond to the acoustic modes and 171 are associated to optical modes. According to Frech and Bates (19), the factor group analysis for stoichiometric Na-β-alumina gives the irreducible representation for the optical modes

$$\Gamma_{opt} = 10\,A_{1g} + 3\,A_{2g} + 12\,B_{1g} + 3\,B_{2g} + 13\,E_{1g} + 15\,E_{2g} + 3\,A_{1u} + 12\,A_{2u} + 3\,B_{1u} + 11\,B_{2u} + 15\,E_{1u} + 14\,E_{2u},$$

where the A_{2u} and E_{1u} modes are IR active and the A_{1g}, E_{1g}, and E_{2g} modes are Raman active, the others being inactive. Accordingly, 27 IR active fundamentals are expected ($12\,A_{2u} + 15\,E_{1u}$). Considering that 54 atoms (22 Al and 32 O) are in the spinel blocks and four atoms (2 Na and 2 O) are located in the mirror planes, assuming the acoustic modes derive from the spinel blocks, we expect 159 optical modes associated to the vibrations of the spinel blocks, giving rise to 23 IR active fundamentals ($10\,A_{2u} + 13\,E_{1u}$). Consequently, four IR active modes ($2\,A_{2u} + 2\,E_{1u}$) are associated with the movements of the ions in the mirror planes. One A_{2u} mode and one E_{1u} mode are associated with the vibrations of the "bridging" oxygen, while also Na ions (Ba ions in our case) are expected to give rise to two IR active modes, $A_{2u} + E_u$ (19, 22).

In conclusion, we expect 23 IR active fundamentals for the vibrations of the spinel blocks, two for the bridging oxygens, and two for nine-fold coordinated mobile Ba^{2+} cations, for the Ba-poor phase of BaAl14.

To separate the motions associated with Al–O bonds from those of the cations lying in the mirror planes we can compare the spectrum of our Ba-β-alumina with that of a defective spinel-type alumina, such as θ-alumina, and of stoichiometric spinels (Fig. 3). In both cases a strong multiple absorption occurs in the region 1000–300 cm^{-1}, but no bands are observed in the region 300–50 cm^{-1}. On the other hand, we can also compare our spectrum with those of other inorganic matrices containing highly uncoordinated Ba cations in cavities, such as cation-exchanged zeolites. It is well known that vibrations associated with these cations lie in the region below 250 cm^{-1}. For example, in the spectra of Ba-exchanged Y zeolite (23), bands at 137, 107, and 55 cm^{-1} have been assigned to the vibrations of Ba ions. Thus, we expect the vibrations of mobile cations in the region below 150 cm^{-1}. Finally, according to Colomban and Lucazeau (22), the two modes associated with the vibrations of the oxygen ions bridging between spinel blocks are expected in the region 300–100 cm^{-1}.

In the spectrum of our BaAl14 sample we observe at least 20 maxima above 300 cm^{-1} (see Fig. 1 and Table 1) and four well resolved bands (with some complexities) in the region 300–50 cm^{-1} (Fig. 2). Considering the possible accidental superimposition of few modes, the spectrum we observe with 24 bands definitely agrees with the structural model discussed above, for which 27 bands were expected. This is also supported by the significant superposition of most of the bands above 300 cm^{-1} with those reported for Na-β-alumina and its analogs (Table 1), assumed to be isostructural. It seems interesting to note that all three Ba-β-aluminas show three main maxima near 760, 560, and 380 cm^{-1}. These maxima roughly correspond to three of the four IR active fundamentals in cubic spinel-type aluminates, $\nu 1$, $\nu 2$, and $\nu 4$, $\nu 3$ being almost superimposed to $\nu 2$, as in the case of $NiAl_2O_4$. They also roughly correspond to the main maxima of the θ-Al_2O_3, which is more complex because, due to its monoclinic structure ($C2/m = C_{2h}^3$ space group), 12 IR-active modes are expected (Fig. 3).

According to Colomban and Lucazeau (22), the lowest frequency mode for monovalent β-aluminas is associated with in-plane movements of the cation (E_{1u} symmetry), while the out-of-plane mode (A_{2u} symmetry) falls at higher frequency and is generally slightly weaker. We can tentatively assign the band at 63 cm^{-1} (with a component near 50 cm^{-1}) to the E_{1u} mode and the band split at 83, 78 cm^{-1} to the A_{2u} mode, both arising from the movements of Ba ions in the mirror planes. Consequently, we can assign the two bands at 139 and 224 cm^{-1} (the last broad) to the movements of bridging oxide ions in the mirror planes (O(5)).

These assignments agree with those of Hayes *et al.* (24, 25) for a Ba-exchanged Na-β''-alumina monocrystal in the region below 150 cm^{-1}. These authors reported a sharp band near 120 cm^{-1}, which they did not discuss, and a

complex of three bands between 80 and 30 cm^{-1}, whose intensity ratios varied strongly with the temperature. They assigned these modes to the movements of Ba^{2+} ions that distribute differently in the two equivalent sublattices as a function of the temperature. The replacement of Na with Ba seem to cause a shift of the bands associated with bridging oxygens from 270 and 211 cm^{-1} (22) to 224 and 130 cm^{-1}, possibly because of the slight increase of the "interblock" distance, reflected in the increase of the cell parameter c (Table 2). The modes associated with Ba movements are observed at slightly lower frequencies compared to those associated to Na movements, in agreement with the greater weight of Ba atoms.

The structure of the Ba-rich phase has been determined by Iyi *et al.* (8) using monocrystals where nearly 20% of Ba is replaced by Pb. On the other hand, the structure determination of our Pb-free BaAl9, performed by the Rietveld analysis of the XRD patterns (16), strongly supports this structure. According to these two studies of the Ba-rich phase, every two "ideal" cells (the same as in Na-β-alumina with Ba replacing Na), each with stoichiometry $2 \times [BaAl_{11}O_{17}]^{+}$, a "defective" cell with stoichiometry $2 \times [Ba_{1.5}Al_{10}O_{17.5}]^{2-}$ occurs, where an interstitial Ba ion (Ba(2)) is located in each "spinel block" with a corresponding one vacant Al (Al(2)) and one vacant oxide ion (O(4)) (8, 16). The two mirror planes are no longer equivalent and this defect is associated with the lack of Ba ions in the mirror plane located between the spinel blocks of the "defective" cell with interstitial barium. Three additional oxygen ions are also located in the "middle oxide" positions (O(6)) in this plane, to balance excess charge, giving rise to a "triple Reidinger defect". This situation occurs with periodicity along the a, b plane giving rise to an $a\sqrt{3} \times a\sqrt{3}$ superstructure with $P\bar{6}m2$ space group (8). However, if we suppose completely random distribution of these defects we can again discuss the structure on the basis of the "standard" hexagonal cell and the $P6_3/mmc$ space group (16). In this case we should expect a spectrum similar to that of the Ba-poor phase.

Actually, the spectrum of BaAl9, constituted by the Ba-rich phase, is distinctly more complex than that of the Ba-poor phase. In the region above 300 cm^{-1} at least 30 components can be found, associated with Al–O movements in the spinel blocks. This agrees with the existing superstructure and/or lower symmetry of the unit cell of the Ba-rich with respect to the Ba-poor phase. Moreover, many prominent features of the Ba-poor phase are not observed at all in the spectrum of the Ba-rich phase (note that the highest frequency bands are all significantly displaced in the two spectra). This confirms that something happened into the spinel blocks, i.e., the insertion of Ba^{2+} ions in interstitial positions.

The spectrum in the 300–50 cm^{-1} region, where the absorptions associated with Ba^{2+} ions and to "bridging" oxygen of the mirror plane are expected (see above), also shows marked differences from that of the Ba-poor phase. According to the above discussion the band with components at 73, 64, and 60 cm^{-1} can be associated with mobile Ba ions in the mirror plane, and are only slightly shifted if compared to the corresponding modes observed for the Ba-poor phase (see above) and to Ba-exchanged β''-alumina (24, 25). The sharp peak at 111 cm^{-1}, not found at all in the spectrum of the Ba-poor phase, can be assigned to vibrations of the "interstitial" Ba ions (Ba(2)) in the spinel blocks. Its clear asymmetry toward lower frequency could be evidence of a second component near 105 cm^{-1}: in fact, two IR-active modes are expected ($A_{2u} + E_{1u}$). The position of these modes at higher frequencies with respect to those assigned to mobile Ba ions agrees with the shorter Ba–O bonds for "interstitial" 12-fold coordinated Ba (mean Ba–O distance 2.825 Å) compared to the mobile 9-fold coordinate Ba (mean Ba–O distance 2.927 Å (16)). The peaks assigned above to "bridging" oxygens in the mirror planes (235 and 139 cm^{-1}) are slightly sharper and only one is definitely although slightly shifted with respect to the Ba-poor spectrum.

The spectrum of the BaAl12 sample can be interpreted as due to the superimposition of the spectra of the BaAl9 and BaAl14 samples, as is very evident for the highest frequency spinel modes in the 1100–900 cm^{-1} region where the bands of both phases are clearly well resolved. Similarly, in the low frequency region (300–50 cm^{-1}), the peaks assigned to Ba ions in the mirror plane show a maximum at 67 cm^{-1} with pronounced components at 75 and 82 cm^{-1}. At higher frequency, the peaks associated with interstitial Ba ions and with bridging oxygen of the Ba-rich phase (112 and 235 cm^{-1}) are very prominent, but that of bridging oxygen of the Ba-poor phase (224 cm^{-1}) is also evident as a pronounced shoulder. This definitely shows that this mterial is actually an intergrowth of domains of the Ba-rich and Ba-poor phases, as already proposed on the basis of XRD measurements (16) and in agreement also with literature data (8).

The IR and FIR spectra of $BaFe_{12}O_{19}$ and, for comparison, of γ-Fe_2O_3 and of the normal spinel $ZnFe_2O_4$ are reported in Fig. 4. The difference between the magnetoplumbite structure and the ideal β-alumina structure lies in the mirror planes. In the mirror planes of magnetoplumbite-type compounds only one-fourth of the oxide ions are missing, and its ccp position is occupied by a large bivalent ion (Ba^{2+} in this case). Moreover, one trivalent ion (Fe(5)) is also located in the "mirror plane" in the "ideal" magnetoplumbite structure in a trigonal bipyramidal coordination sphere. However, according to Obradors *et al.* (21), this Fe^{3+} ion in $BaFe_{12}O_{19}$ is dynami-

cally disordered between two positions slightly above or below the mirror plane.

Thus, the structure of $BaFe_{12}O_{19}$ is constituted by $[Fe_{11}O_{16}]^+$ spinel blocks separated by $[BaFeO_3]^-$ layers. Factor group analysis obtains the irreducible representation for the optical modes of ideal $BaFe_{12}O_{19}$

$$\Gamma_{opt} = 13\,A_{1g} + 3\,A_{2g} + 10\,B_{1g} + 5\,B_{2g} + 18\,E_{1g} + 13\,E_{2g} + 4\,A_{1u} + 13\,A_{2u} + 5\,B_{1u} + 10\,B_{2u} + 18\,E_{1u} + 13\,E_{2u}$$

with 31 IR active modes ($13\,A_{2u} + 18\,E_{1u}$) and 44 Raman active modes ($13\,A_{1g} + 18\,E_{1g} + 13\,E_{2g}$).

From the spectrum of Fig. 3, only 14 components are observed. Most of them closely correspond to the E_{1u} fundamental TO modes as determined by the monocrystal reflection measurements by Nikolic *et al.* (26), reported in Table 4. These authors only observed 10 of the 18 E_{1u} fundamentals and were unable to measure the A_{2u} fundamentals, due to the size of their monocrystal. The spectrum of Fig. 4, which closely resembles the reflection spectrum reported by Nikolic *et al.* (26), contains three predominant and certainly complex absorptions in the region 800–200 cm^{-1}. The main maxima roughly correspond to the three main maxima observed in the spectrum of the normal spinel $ZnFe_2O_4$, as well as to the three most intense maxima observed in the spectrum of γ-Fe_2O_3 (maghemite), both also shown in Fig. 4 for comparison. Moreover, all three spectra show one sharp and weak band in the region 160–180 cm^{-1}. The spectrum of $ZnFe_2O_4$ is very simple because spinel-type compounds ($Fd3m$ point group, with three molecular units per smallest Bravais cell) only have four IR active models (F_{1u}) (27). In contrast, γ-Fe_2O_3 has a more complex spectrum: we observe nearly 20 components, which could agree with the $P4_132 = O^7$ space group with 8 molecular units per unit cell of partially ordered γ-Fe_2O_3, for which 21 IR active fundamentals are expected. Instead, it contrasts with the fully ordered defective tetragonal superstructure ($P4_32_12 = D_8^4$ space group, with 32 molecular units per unit cell), for which 179 IR active modes are expected (28). On the basis of the comparison of the spectra of these three ferrite compounds, it seems obvious that all bands observed in the region 800–160 cm^{-1} arise from Fe–O vibrations and are generated by splittings and activation in the IR of the fundamentals of cubic spinels such as $ZnFe_2O_4$. In Table 4 the Raman peaks observed for $ZnFe_2O_4$ and γ-Fe_2O_3 are also reported and show that all detectable fundamentals in these cases lie above 160 cm^{-1}.

TABLE 4
Position (cm^{-1}) of the Skeletal Bands of $BaFe_{12}O_{19}$ and of Reference Spinel-Type Ferrites

$ZnFe_2O_4$ Ref. (30)		γ-Fe_2O_3 Ref. (29)		$BaFe_{12}O_{19}$ E_{1u} fundamentals		
					Monocrystal Ref. (26)	
IR	Raman	IR	Raman	Powder This work	TO	LO
		725				
		694	706			
	645	635	660			
541		551	560	585	585	690
	500		502	543	545	550
		480				
	460	441	455			
		420		438	430	480
380		390		401		
		364	380	360	362	364
	350	351		338	333	351
		325	330	323		
313		304		302	300	313
		261	280	284	285	290
		232	260	250	248	252
		210		212		
	175		186			
166		180		177	177	180
				124		
				102	95	96

$BaFe_{12}O_{19}$ shows an additional strong absorption in the region 150–50 cm^{-1}, which we observe split at 124, 102 cm^{-1}. This absorption can be assigned to vibrations of Ba^{2+} cations, which in fact contribute with two IR active fundamentals ($A_{2u} + E_{1u}$) to the vibrational structure of this solid. The lower energy mode (102 cm^{-1}) could correspond to the E_{1u} fundamental observed at 95 cm^{-1} by Nikolic *et al.* (26), while the higher frequency one, not observed by these authors, should consequently be due to the A_{2u} component.

It seems interesting to note that these modes fall at very similar frequencies to the modes assigned to the vibrations of the "interstitial" Ba ions in Ba-rich Ba-β-alumina (111, 105 cm^{-1}). Accordingly, in both cases Ba is in a 12-fold coordination, with similar Ba–O distances near 2.85 Å. For comparison, Ba vibrations in the YBCO superconductor give rise to two IR bands in the same region (114, 104 cm^{-1} (31)) although in this case its overall coordination is 10-fold, but the mean Ba–O distance is again about 2.85 Å. The vibrational frequencies associated with mobile Ba ions located in the β-alumina mirror planes (80–50 cm^{-1}) fall to much lower values, showing the strong effect of its lower overall coordination and longer Ba–O mean distance.

One further striking feature is the breadth of the spectrum of $BaFe_{12}O_{19}$ in the "spinel block" region, where many components are certainly lost because of their par-

tial superimposition and, probably, their greater width. This does not occur in the spectra of β-aluminas, whose components are sharp and well resolved. It cannot be due to the character of Fe–O bonds, because of the presence of very definite components in the spectrum of γ-Fe_2O_3 (Fig. 3). Moreover, it is not a property of our powder, because the same effect has been observed by Nikolic *et al.* (26) in single crystals. It may be the result of the dynamic disorder of Fe(5) ions, distributed between the 2d "in plane" sites and the two 4e "out of plane" sites, as discussed by Obradors *et al.* (21). Moreover, it is known that these hexagonal ferrites generally contain large numbers of lattice defects, which could justify the much lower coercive fields measured experimentally (3000–4000 Oe) compared to the theoretical values (17,000 Oe) (12). These defects, associated with magnetic Fe ions, can contribute to increased disorder and to loose resolution of the fundamental skeletal modes.

CONCLUSIONS

The analysis of the skeletal IR spectra of Ba-β-aluminas and Ba-ferrite has been discussed in relation to the structural features of these materials. In particular:

(a) The spectrum of the sample with composition $BaAl_{14}O_{22}$ composed by the Ba-poor β-alumina phase agrees with the structural features proposed for this phase, considered to be similar to those of Na-β-alumina with random defects to compensate for the excess charge of Ba^{2+} ions.

(b) The spectrum of the sample with composition $BaAl_9O_{14.5}$ composed by the Ba-rich β-alumina phase definitely supports the existence of a superstructure (because of the larger number of observed modes) and agrees with the presence of interstitial Ba ions in the spinel blocks, as proposed in previous papers on the basis of diffraction data.

(c) The spectrum of the sample with composition $BaAl_{12}O_{19}$ confirms the existence of domains of both Ba-rich and Ba-poor β-alumina phases.

(d) The spectrum of a $BaFe_{12}O_{19}$ sample agrees with the features of the magnetoplumbite-type structure but its comparison with the spectra of monocrystals with the same composition suggests that many defects and much disorder occurs in this solid with broadening and averaging of several fundamental modes.

ACKNOWLEDGMENTS

This work was supported by MURST (national group "Struttura e reattività delle superfici").

REFERENCES

1. A. R. West, "Solid State Chemistry and Its Applications," Wiley, New York, 1984.
2. C. A. Beevers and M. A. S. Ross, *Z. Kristallogr.* **97,** 59 (1937).
3. C. R. Peters, M. Bettman, J. W. Moore, and M. D. Gluck, *Acta. Crystallogr. Sect. B* **27,** 1826 (1971).
4. A. L. N. Stevels and A. D. M. Schrama-de Pauw, *J. Electrochem. Soc.* **123,** 690 (1976).
5. J. Kirchnerova and C. W. Bale, *Mater. Res. Bull.* **25,** 389 (1990).
6. J. Dexpert-Ghys, M. Faucher, and P. Caro, *J. Solid State Chem.* **19,** 193 (1976).
7. F. P. F. Van Berkel, H. W. Zandbergen, G. C. Vershoor, and D. J. W. Ijdo, *Acta Crystallogr. Sect. C* **40,** 1124 (1984).
8. N. Iyi, Z. Inoue, S. Takekawa, and S. Kimura, *J. Solid State Chem.* **60,** 41 (1985).
9. M. Machida, K. Eguchi, and H. Arai, *J. Am. Ceram. Soc.* **71,** 1142 (1988).
10. A. Kato, H. Yamashita, and S. Matsuda, *in* "Successful Design of Catalysts" (T. Inui, Ed.), p. 25. Elsevier, Amsterdam, 1988.
11. G. J. Dudley and B. C. H. Steele, *J. Solid State Chem.* **21,** 1 (1977).
12. W. Buchner, R. Schliebs, G. Winter, and K. H. Buchel, "Industrial Inorganic Chemistry." VCH, Weinheim, 1989.
13. A. Rafaoui, A. Kahn, J. Théry, and D. Vivien, *Solid State Ionics* **9–10,** 331 (1983).
14. S. Nariki, S. Ito, and N. Yoneda, *J. Solid State Chem.* **87,** 159 (1990).
15. V. Delacarte, A. Kahn-Harari, and J. Théry, *Mater. Res. Bull.* **28,** 435 (1993).
16. G. Groppi, M. Bellotto, C. Cristiani, P. Forzatti, and P. L. Villa, *Appl. Catal.* **104,** 101 (1993).
17. G. Groppi, F. Assandri, M. Bellotto, C. Cristiani, and P. Forzatti, *J. Solid State Chem.* **114,** 326 (1995).
18. G. Busca, C. Cristiani, G. Groppi, and P. Forzatti, *Catal. Lett.* **31,** 65 (1995).
19. R. Frech and J. B. Bates, *Spectrochim. Acta Part A* **35,** 685 (1979).
20. A. S. Barker, J. A. Ditzenberger, and J. P. Renneika, *Phys. Rev. B* **14,** 386 (1976).
21. X. Obradors, A. Collomb, M. Pernet, D. Samaras, and J. C. Joubert, *J. Solid State Chem.* **56,** 171 (1985).
22. Ph. Colomban and G. Lucazeau, *J. Chem. Phys.* **72,** 1213 (1980).
23. W. M. Bulter, C. L. Angell, M. McAllieter, and W. M. Risen, *J. Phys. Chem.* **81,** 2061 (1977).
24. W. Hayes, K. Kjaer, F. L. Pratt, and B. Schonfeld, *J. Phys. C Solid State Phys.* **18,** L567 (1985).
25. W. Hayes and F. L. Pratt, *J. Phys. C Solid State Phys.* **19,** 929 (1986).
26. P. M. Nikolic, Lj. Zivanov, O. S. Aleksic, D. Samaras, G. A. Gledhill, and J. D. Collins, *Infrared Phys.* **30,** 265 (1990).
27. W. B. White and B. DeAngelis, *Spectrochim. Acta Part A* **23,** 985 (1967).
28. M. P. Morales, C. Pecharroman, T. Gonzales Carreno, and C. J. Serna, *J. Solid State Chem.* **108,** 158 (1994).
29. M. I. Baraton, G. Busca, V. Lorenzelli, and R. J. Willey, *J. Mater. Sci. Lett.* **13,** 275 (1994).
30. G. Busca, M. Daturi, G. Oliveri, E. Kotur, and R. J. Willey, *in* "Preparation of Catalysts VI" (G. Poncelet and B. Delmon, Eds.). Elsevier, Amsterdam, 1994, in press.
31. M. Daturi, G. Busca, M. Magnone, and M. Ferretti, submitted for publication.